Journal of the European Ceramic Society 22 (2002) 639–652

www.elsevier.com/locate/jeurceramsoc

Reinforcement of single-firing ceramic glazes with the addition of polycrystalline tetragonal zirconia (3Y–TZP) or zircon

M. Llusar[a,*], C. Rodrigues[b], J. Labrincha[c], M. Flores[d], G. Monrós[a]

[a]*U.P. de Química Inorgànica i Orgànica, Universitat Jaume I, 12071 Castellón, Spain*
[b]*ESTG, Instituto Politécnico de Viana do Castelo, 4900 Viana do Castelo, Portugal*
[c]*Departamento de Engenharia Cerâmica e do Vidro, UIMC, Universidade de Aveiro, 3810 Aveiro, Portugal*
[d]*Esmalglass, S. A., Portugal*

Received 16 February 2001; received in revised form 24 April 2001; accepted 20 May 2001

Abstract

The addition of fine-grained polycrystalline tetragonal zirconia (3%Y_2O_3–TZP, or 3Y–TZP) to conventional, single-firing, ceramic glazes was studied with the aim to enhance their hardness, fracture toughness and wear resistance for floor tile applications. The stability of the added tetragonal zirconia towards solution in the glaze and/or zircon crystallization was found strongly dependent on glaze composition, firing treatment, and on the way of preparing the samples (uniaxially-pressed pellets or thin-layer coatings). 3Y–TZP remained stable in fast-fired pellets, but partial crystallization of prismatic zircon microcrystals (2–3 μm) occurred in samples prepared as thin-layer coatings. Addition of 10–30 wt.% of 3Y–TZP to a conventional single-firing glaze that was industrially enameled (thin films) onto low-porous floor tiles, promoted an important enhancement of Vickers microhardness (H_v from 6.0 to 8.4 GPa), fracture toughness (K_{IC} from 1.35 to 2.23 MPa $m^{1/2}$), and wear resistance (PEI abrasion number from 2 to 5). The achieved reinforcement was higher with 3Y–TZP than with zircon addition, and must be attributed to the stress-induced transformation-toughening mechanism promoted by the undissolved stabilized tetragonal zirconia, and also to partial zircon crystallization. The possibility of obtaining ceramic coatings mechanically reinforced with 3Y–TZP additions, while also maintaining a glossy aspect, was also confirmed. © 2002 Published by Elsevier Science Ltd.

Keywords: Fracture; Glazes; Hardness; TZP; Wear resistance; ZrO_2; $ZrSiO_4$

1. Introduction

Mechanical properties of brittle materials can be improved by the introduction of metastable tetragonal zirconia particles, either added or precipitated in situ during the annealing treatment.[1] The tetragonal-to-monoclinic martensitic transformation of zirconia grains is accompanied by volume and shear strains which can act to counteract the tensile stress field generated at the tip of a propagating crack, resulting in an enhancement of fracture resistance or toughness. The tetragonal polymorph of zirconia can be stabilized at room temperature by appropriate doping with oxides such as CaO, MgO, Y_2O_3, CeO_2, etc., and depending on the type and content of doping oxide, fully-stabilized zirconia (FSZ), partially-stabilized zirconia (PSZ), or fine-grained polycrystalline tetragonal zirconia (TZP) are obtained. These stabilized zirconias, especially yttrium-doped TZP because of its good mechanical properties (high flexural strength, hardness, and fracture toughness),[2–4] are widely used to prepare composite materials with optimal tribological properties in both ceramic[5,6] or glassy matrices. The glassy matrix which has received deeper attention is based on silica, and, in this case, tetragonal zirconia precipitation has been observed during the calcination of gels,[7,8] or during the crystallization of glasses of the system ZrO_2–SiO_2.[9]

However, much less attention has been devoted to the introduction of stabilized zirconia in more complex vitreous systems as those employed in the formulation of ceramic glazes for wall and floor tiles. Formulations of ceramic glazes, composed by a mixture of a wide number of acid (SiO_2, B_2O_3, ZrO_2, TiO_2), basic (Na_2O, K_2O, MgO, CaO, BaO, ZnO, PbO) and amphotere (Al_2O_3) oxides, are carefully developed or tailor-made to satisfy both aesthetical (gloss, transparency or opacity,

* Corresponding author. Tel.: +34-964-728234; fax: +34-964-728214.
E-mail address: mllusar@qio.uji.es (M. Llusar).

0955-2219/02/$ - see front matter © 2002 Published by Elsevier Science Ltd.
PII: S0955-2219(01)00339-9

color, etc) and technical requirements (compatibility with the clay tile and with the firing schedule, chemical resistance, and good mechanical properties to withstand severe wear, stress and/or impact conditions derived from use, etc). Usually, reinforcement of ceramic glazes is obtained either with the addition of highly refractory crystalline phases of high hardness and/or strength values (corundum, mullite, zircon, rutile, β-spodumene, andalucite) which remain insoluble and stable in the glassy matrix, or with the in situ devitrification of the reinforcement phase (zircon, diopside, β-spodumene) during glaze annealing.[10,11] Instead of tetragonal zirconia, monoclinic zirconia (*m*-ZrO_2, or baddeleyite) is commonly employed in complex ceramic glaze formulations as a nucleation agent,[12] with the aim to promote zircon devitrification, which confers opacity and/or an improvement of mechanical properties. Concerning the use of stabilized tetragonal zirconia, Höche et al.[13] reported the beneficial effects on mechanical properties of the formation of transformable tetragonal ZrO_2 in glass-ceramics belonging to the system MgO–CaO–Al_2O_3–SiO_2 doped with N and ZrO_2. Generali et al.[14] studied the M_2O–CaO–ZrO_2–SiO_2 glass–ceramic system (with M = Li, Na, and K), and found that tetragonal zirconia precipitates were not stable enough, due to the strong tendency for devitrification of Ca–Zr silicate ($2CaO{\cdot}4SiO_2{\cdot}ZrO_2$). The low stability of tetragonal zirconia was also corroborated by Monrós et al.[15] when introducing Ca-partially-stabilized zirconia (Ca-PSZ) obtained by sol-gel procedures in the formulation of conventional ceramic glazes.

With respect to the difficulties to accomplish an in situ devitrification process of tetragonal zirconia precipitates having the appropriated morphology and size, the direct addition of stabilized tetragonal zirconia to the glaze can be an alternative way to achieve optimal conditions, in terms of composition, microstructure and/or morphology. By using this method, an improvement of the mechanical properties of the ceramic glaze is observed. Unfortunately, tetragonal zirconia and dopant ions (Ca, Mg, Y, etc.) readily react with molten ceramic glazes during the firing treatment, being dissoluted or incorporated in to the glassy phase. Studies performed on the stability of zirconia-based oxygen sensors in molten glazes show that Ca and Mg are more easily dissolved than Y.[16,17] Leaching stabilizing ions out of the glass results in a progressive destabilization of tetragonal zirconia, and the transformation into the monoclinic form (*m*-ZrO_2) gives rise to a degradation of the mechanical properties. Addition of yttrium-stabilized tetragonal zirconia seems to be highly more efficient to enhance the mechanical properties of ceramic glazes than Ca- and/or Mg-doped zirconia.

The current work explores the use of yttrium-stabilized polycrystalline tetragonal zirconia (3Y–TZP) as a mechanically reinforcing additive of conventional single-firing ceramic glazes. Single-firing ceramic glazes coated onto floor or wall tiles are normally fired at temperatures around 1100–1200 °C in single and fast thermal cycles of about 50 min (or less). In such rapid conditions, solution of tetragonal zirconia grains in the melt and/or zircon devitrification could not be fully completed, and a significant amount of transformable tetragonal zirconia could remain undissolved and be effective in toughening the ceramic glaze.

2. Experimental

2.1. Raw materials

A commercial polycrystalline tetragonal zirconia stabilized with 3 mol% of yttrium (3Y–TZP) supplied by Tosoh Corporation was selected to be added to conventional single-firing ceramic glazes formulations. This powder consists in spherical agglomerates (granules) of sizes between 5 and 40 μm, being compressed the dominant fraction between 10 and 20 μm. The typical crystallite size is about 25 nm, and the specific surface area (estimated by BET analysis) is 16 m^2/g. XRD analysis of 3Y–TZP powder indicated the presence of a minor quantity of monoclinic zirconia in addition to the tetragonal grains (the approximate monoclinic phase content was estimated around 8 wt.%).

A coarse zircon powder ($ZrSiO_4$) commonly used in the glaze industry (known as Zircosil-300, or ZS-300, and supplied by NIX Cristal) was also added to glazes that were coated by following a typical industrial procedure, detailed later in this work, in order to compare with *t*-ZrO_2 induced effects. The mean grain size of the ZS-300 powder is about 9 μm, with 90 wt.% of particles below 30 μm, and 60 wt.% below 13 μm.

Two representative formulations of conventional single-firing transparent ceramic glazes, supplied by Esmalglass, S.A. and referenced as L and H, were selected for the present study. Both glazes were used as frits (previously melted at higher temperatures and quenched in water to room temperature to obtain an amorphous glass). The approximate oxide composition (wt.%) of both ceramic glazes can be seen in Table 1. Glaze H has considerably higher silica content, while glaze L is Al_2O_3- and B_2O_3-richer (absent in glaze H). Due to the higher amounts of B_2O_3 and earth-alkaline oxides, glaze L melts at a considerably lower temperature than glaze H (melting temperature around 1150 and 1240 °C, respectively).

2.2. Sample preparation

Samples were prepared in two different ways: (i) pellets and (ii) industrially produced film coatings. In the preliminary studies, cylindrical pellets (2 cm of diameter)

Table 1
Approximate oxide composition (wt.%) of the transparent ceramic glazes (frits) employed in the study

Frit or glaze	% ($Na_2O + K_2O$)	% (CaO + MgO)	% ZnO	% B_2O_3	% Al_2O_3	% SiO_2
L	6	15	10	3	8	58
H	6	14	9	–	6	65

were obtained by uniaxial pressing of dry powders (4 g/pellet). To obtain a homogeneous distribution of all the raw materials components, both of L and H frits were previously milled in an agate mortar and the fraction below 45 μm was mixed with the corresponding quantity of 3Y–TZP. This operation was carried out in dry conditions and without grinding media to prevent changes in size and morphology of tetragonal zirconia grains, and also to avoid transformation to the monoclinic form, generally induced by grinding.[8,18–23]

In the second part of the study, mixtures of glaze L with different quantities (10, 20 and 30 wt.%) of 3Y–TZP or ZS-300 powders were homogenized in water following two distinct procedures (A and B, described below). Resulting enamel slurries were spray-coated (after reological control) as film layers onto stoneware floor tiles (33×33 cm format) of low porosity, ensuring the application of a constant thickness. In samples homogenized by procedure A, 300 g of the mixture was dispersed in water (150 ml), with some common minor additives (diluted solution of carboxymethylcellulose, CMC, as binder, and Tripolyphosphate, TPF, as deffloculant), and then this batch was electrically stirred during 1–2 min. In procedure B, 300 g of the starting mixture made of glaze (at this time made of coarse and un-milled frit) and 3Y–TZP or ZS-300 powders were ball-milled during 50 min (alumina grinding media), using water (120 ml) as dispersant media, and minor additives (0.06 wt.% of NaCl, 0.15 wt.% of CMC, and 0.15 wt.% of TPF). Method B corresponds to the commonly used process in the ceramic glaze industry, and was adopted in order to assess the possible effect of ball milling process on the stability of the tetragonal zirconia. Optimal reological conditions (viscosity and density) of slurries were adjusted, when necessary, by small additions of water and/or TPF. The density values of the as-prepared slurries changed from 1620 to 1820 g/l, and their viscosity values were kept below 0.14 Pas. All the spray-coated samples were dried at 100 °C during 2 h, and then fired in an industrial furnace.

2.3. Firing schedules

Pellet samples were fired up to 1200 °C in laboratory electrical kilns following two different firing schedules: (i) a slow firing cycle consisting of a 2 h 45 min heating ramp up to 1200 °C, a soaking time of 1 h at this temperature, and a slow cooling down of 4–5 h to room temperature, and (ii) a 51 min fast-firing cycle (industrial schedule) with a 20 min heating ramp up to 1200 °C, a 5 min soaking time at this temperature, and a 19 min cooling down to room temperature.

Industrially deposited samples onto floor tiles were single-fired (green bisque and glaze layer at once in a single cycle), following a 42 min fast cycle in a roller single-layer industrial furnace. This cycle consisted of a 20 min heating ramp until 1200 °C, followed by a soaking period of 5 min at maximum temperature, and then a cooling step of 17 min to room temperature.

2.4. Characterization techniques

X-ray diffraction (XRD) of the fired pellets and industrial vitro-crystalline coatings was carried out with a Rigaku diffractometer using Ni filtered CuK_α radiation, in order to assess the stability of the tetragonal zirconia towards dissolution in the glaze and/or the zircon devitrification processes. Further information was obtained by scanning electron microscopy (SEM) characterization of the samples, performed with a Hitachi S4100 electron microscope equipped with EDX analysis. Pellet samples were cut in thin layers, polished with diamond paste and C-graphite sputtered prior to SEM observation.

The mechanical properties (Vickers microhardness: H_v, fracture toughness: K_{IC}, and abrasion resistance) of the industrially coated glazes onto tiles were also measured. To estimate H_v values, 5–7 indentations were made on different regions of each sample by applying a load of 9.8 N (pure glaze samples were indented at a lower load of 4.9 N). A Shimadzu-M micro-hardness indenter was used. The length of the indentation diagonals ($2a$) and of the cracks (l) generated from each indentation apex were measured by using an optical microscope. The fracture toughness, K_{IC}, was calculated from Niihara et al.'s relationship[24] which is valid when the crack-to-indent ratio (l/a) is inferior to 2.5:

$$K_{IC} = 0.055 H_v a^{1/2} (l/a)^{-1/2}$$

The abrasion resistance of enameled samples was determined using a standarized test (International Standard ISO 10545-7), widely known as PEI abrasion test. The principle of this method is based on rotation of an abrasive load (steel balls of different diameters) on the surface of the sample (glazed tile), and on the

assessment of the wear level by means of visual comparison of abraded and non-abraded tiles. According to the number of revolutions necessary to produce a visible abrasion failure, samples are classified from PEI class 0 (lowest abrasion resistance) to PEI class 5 (highest abrasion resistance, that also requires that samples have passed the test specified in ISO 10545-14 for resistance to stains).

Finally, selected optical properties (gloss and transparence/opacity) of the glaze coatings were also measured. The gloss (60° geometry) was measured with a Multi-Gloss 268 Minolta Reflectometer, following standard procedures (DIN 67 530, ISO 2813, ASTM D 523, and BS 3900 Part D5), while transparency or opacity was determined by measuring the whiteness index (ASTM 1925) with a Perkin Elmer spectrophotometer. The whiteness index can be easily correlated with the opacity, since the lower this index, the whiter and the more opaque is the sample.

3. Results

3.1. Preliminary studies with pellet samples

To analyze the effect of glaze composition and melting temperature on 3Y–TZP stability, several pellets of both glazes (L and H) were prepared, containing or not 10 wt.% of zirconia-based powder. These pellets were fired at 1200 °C following a very long cycle (8–9 h).

Pure glaze pellets remained amorphous (non-crystalline) after the firing treatment (as expected for transparent glazes). According to XRD results (see Fig. 1a–c) 3Y–TZP stability was found much higher in glaze H. In fact, the reaction between zirconia-based material and glaze L (more fusible) was almost complete. In a first step, martensitic-type transformation to the monoclinic structure must have occurred followed by the solution on glaze and reaction with silica to give zircon ($ZrSiO_4$). In glaze H, however, XRD characterization still shows the presence of a large amount of unreacted (stabilized) 3Y–TZP, despite the appearance of zircon and the presence of small amounts of *m*-ZrO_2. These observations clearly denote an incomplete reaction between 3Y–TZP and H glaze phases. SEM analyses confirmed these results. In glaze L the original 3Y–TZP granules still visible (Fig. 2a) are almost completely transformed in fractured zircon monoliths (labeled as Z) surrounded by fine rounded-shaped monoclinic zirconia grains. Those grains (labeled as M) are better seen at a higher magnification ratio (Fig. 2b and c). Fig. 2d shows EDX spot analysis of a zircon grain. The presence of inter- and intra-granular cracks (indicated with black arrows in Fig. 2a) could be due to the volume expansion associated with zircon formation and/or with the *t*-to-*m* martensitic transformation of ZrO_2. Microcracking could also be due to the stabilized crystalline phases (ZrO_2 and $ZrSiO_4$) having a thermal expansion substantially different from that of the residual glaze, or to the anisotropy of thermal expansion of larger $ZrSiO_4$ grains. On the contrary, in glaze H the newly formed monolithic zircon grains are much rare and seems to correspond to an early formation stage (as can be seen at the bottom of the SEM detail presented in Fig 2c).

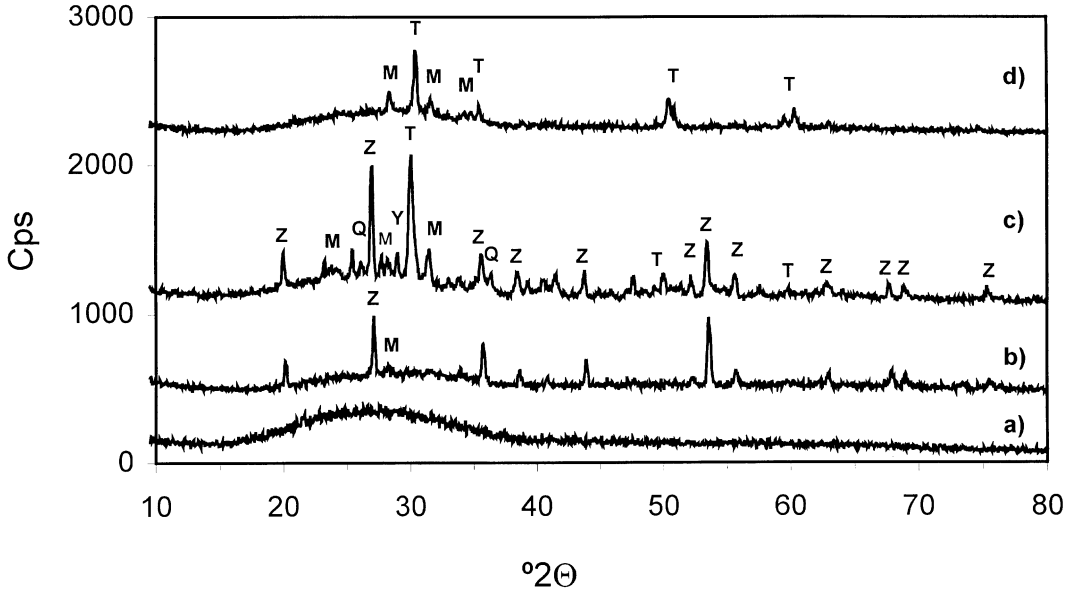

Fig. 1. XRD patterns corresponding to fired pellet samples: (a) slow-fired glaze L, (b) slow-fired glaze L + 10 wt.% 3Y–TZP, (c) slow-fired glaze H + 10 wt.% 3Y–TZP, and (d) fast-fired glaze L + 10 wt.% 3Y–TZP. Crystalline phases: *T* (tetragonal ZrO_2), *M* (monoclinic ZrO_2), *Z* ($ZrSiO_4$), *Q* (quartz), and *Y* (Y_2O_3).

Therefore, differences in composition of the ceramic glaze (higher silica content and absence of boron oxide in glaze H, etc.) and in the melting temperature (glaze H shows higher refractoriness) cause important effects on the stabilization of polycrystalline tetragonal zirconia (higher stability in glaze H than in glaze L). Further studies should be conducted to better understand the contribution of both individual oxides and melting temperature to such stabilization (research which is beyond the scope of the present study).

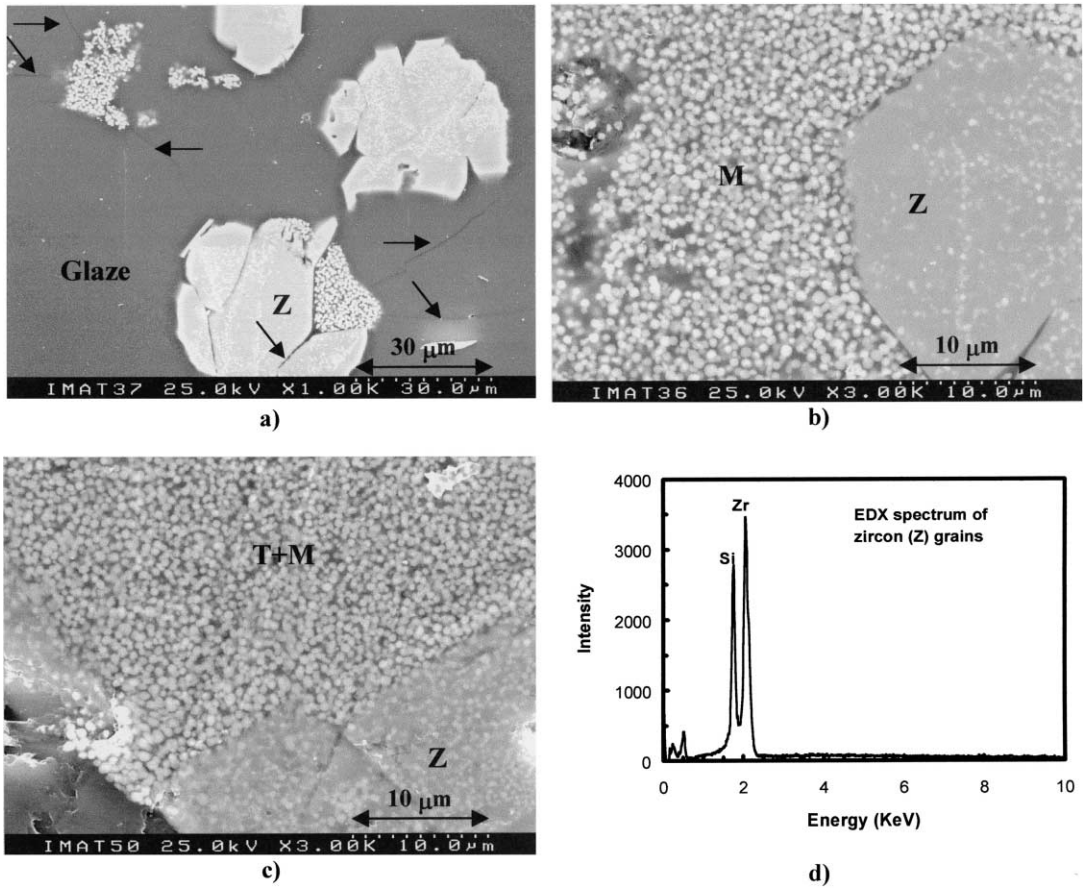

Fig. 2. SEM micrographs of slow-fired (8–9 h cycle) pellets obtained with a 10 wt.% addition of 3Y–TZP to glaze L [(a) at a magnification of 1000, and (b) at a magnification of 3000] and to glaze H [(c) at a magnification of 3000], and EDX spectrum (d) obtained on analyzing the grain labeled as Z (zircon crystallization). Inter- and intra-granular cracks are indicated with arrows. *M* and *T* labels refer to *m*- and *t*-zirconia grains.

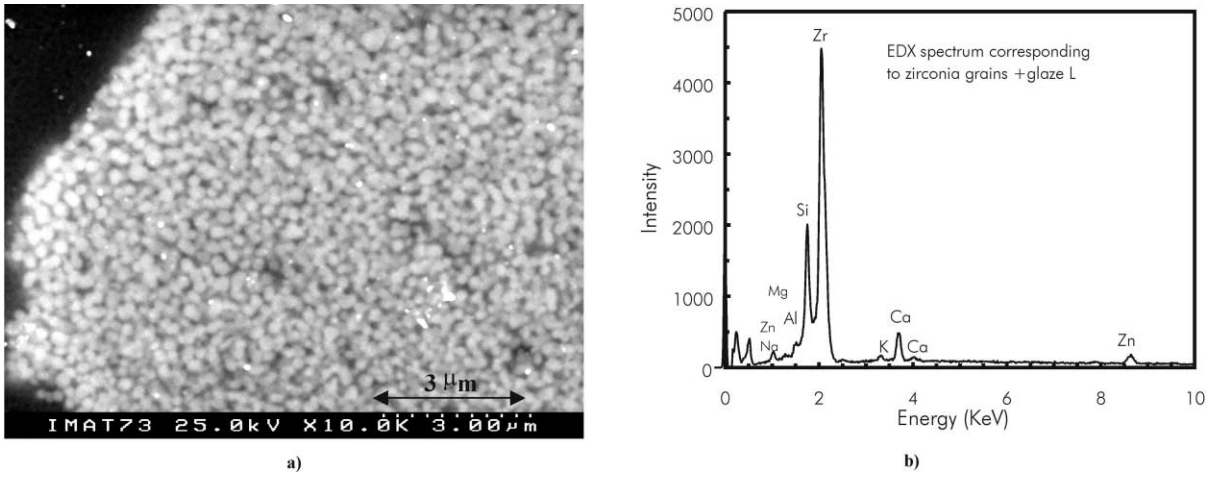

Fig. 3. SEM micrograph (a) and EDX spectrum (b) of a detail of the pellet obtained with a 10 wt.% addition of 3Y–TZP to glaze L fired to 1200 °C with a rapid cycle (51 min). The image shows the fine (0.3 μm) and round-shaped grains of *t*-ZrO_2 (constituting the 3Y–TZP spherical aggregates) that still have not been solved in the glaze or reacted to form zircon.

To analyze the effect of firing treatment duration, a pellet made of 10 wt.% of 3Y–TZP + glaze L was fast-fired up to 1200 °C during only 51 mi This firing schedule is similar to that employed in industrial processes. In such rapid thermal cycles, it is more probable that 3Y–TZP will be kept stable and less formation of zircon would be expected. Effectively, XRD characterization (see Fig. 1d) confirms that an important amount of tetragonal zirconia remains in the pellet after this firing, without the occurrence of either martensitic-type transformation to monoclinic zirconia (a similar *m*-ZrO_2 content to that of the 3Y–TZP raw material was observed) or zircon crystallization. The absence of zircon crystals was also confirmed by SEM, since only spherical 3Y–TZP aggregates made of fine (0.3 μm) rounded-shaped grains are seen (see Fig. 3a, and the corresponding EDX spectrum in Fig. 3b). Therefore, even in those ceramic glazes in which the tetragonal zirconia phase is less stable (glaze L), the use of rapid firing schedules allowed to obtain vitro-crystalline glazes mostly consisting of fine-grained and stabilized (undissolved) tetragonal zirconia.

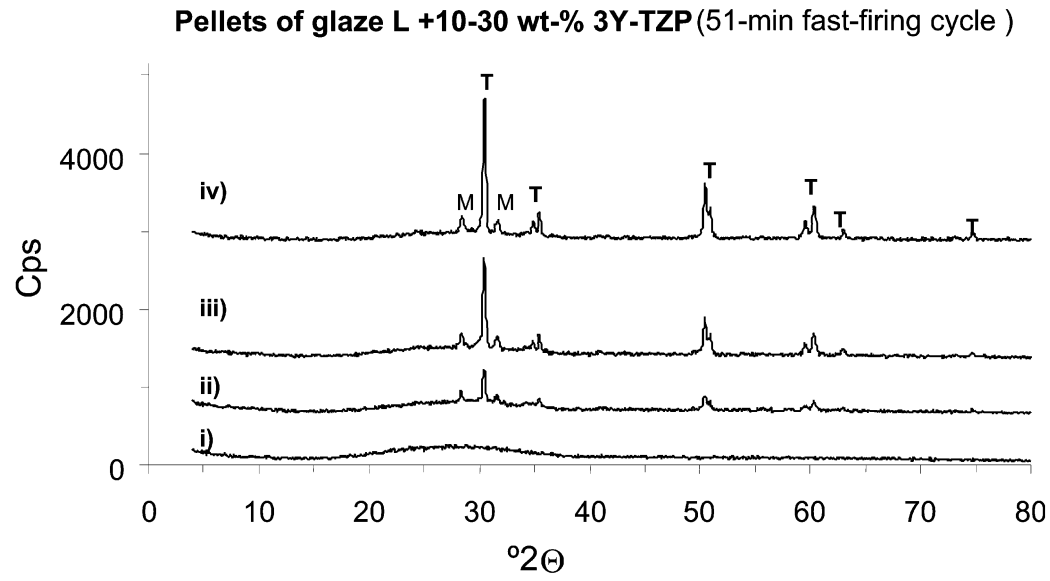

a)

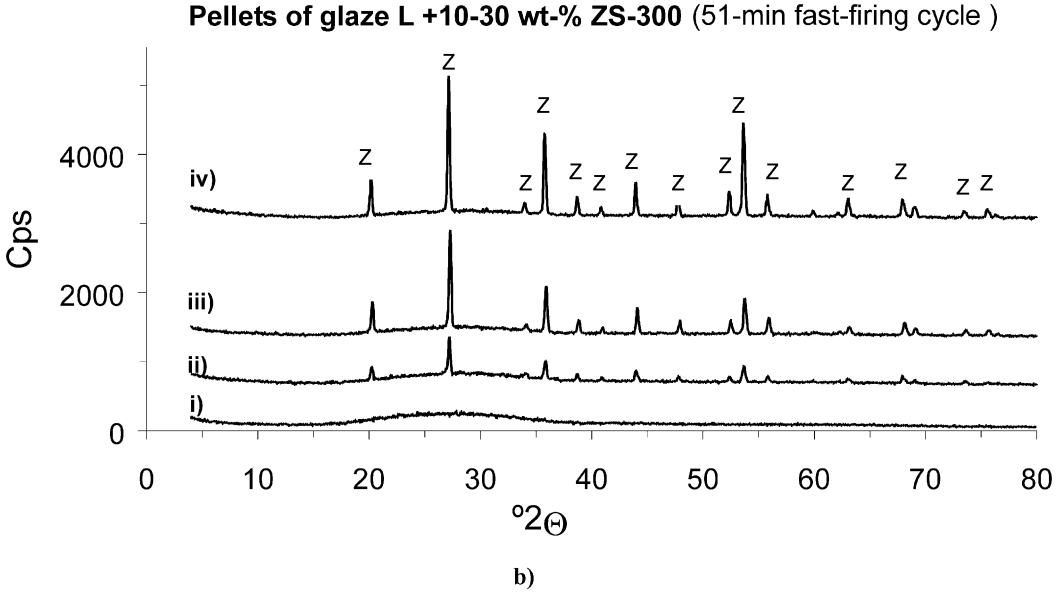

b)

Fig. 4. XRD patterns corresponding to fast-fired (51-min cycle) pellets of glaze L with additions of 0 (i), 10 (ii), 20 (iii) and 30 (iv) wt.% of 3Y–TZP (a) or of ZS-300 (b). Crystalline phases: *T* (tetragonal ZrO_2), *M* (monoclinic ZrO_2), and *Z* (zircon, $ZrSiO_4$).

Glaze L was then selected in the second part of the study to conduct industrial fast-firing tests, preparing the samples as film coatings. Prior to the realization of the industrial tests, pellets with increasing amounts (10, 20 and 30 wt.%) of 3Y–TZP or zircon (ZS-300) were prepared and fired in a laboratory-scale electrical furnace following the same rapid cycle (51 min). These tests served as comparison between pellet samples and industrially prepared coatings, since the stability of tetragonal zirconia grains added is expected to be rather different in both cases, due to differences in diffusion processes, exposure to kiln atmosphere, and interfacial contact between grains and glaze. XRD patterns of the fast-fired pellets (see Fig. 4a and b) shows that both 3Y–TZP and zircon phases remain stable, irrespective of the addition level. Moreover, the XRD peaks area of added crystalline phases (t-ZrO_2 and $ZrSiO_4$) is observed to rise in correlation with their amounts.

3.2. Industrial tests with fast-fired industrial coatings

According to the experimental methodology described in Section 2.2, two different series of samples (A and B) were prepared as film coatings having several contents of 3Y–TZP or ZS-300, which were coated onto low-porous floor tiles. As-prepared samples were referenced as shown in Table 2. Fast-fired coatings were characterized by XRD and by SEM/EDX techniques. Mechanical and optical properties were also measured.

3.2.1. XRD characterization

XRD patterns of fast-fired coatings are given in Figs. 5 and 6. The reactivity of 3Y–TZP towards the molten glaze was found much higher in fast-fired coatings than in the homologous pellet samples (cf. Figs. 5 and 4a). On the contrary, zircon-doped samples seem to exhibit similar stability towards the glaze (linear trends are observed between zircon peaks area and the added amount), irrespective of the preparation method (either pellets—Fig. 4b, or coatings—Fig. 6) and of the homogenization procedure (compare Fig. 6a and b). For 3Y–TZP doped coatings (Fig. 5), significant zircon crystallization occurred. Samples with doping levels up to 20 wt.% show more intense zircon XRD peaks than those of tetragonal zirconia, and stable crystals of this doping agent (neither dissolved in the glaze nor reacted with silica to form zircon) are only dominant for high addition levels (30 wt.%). The lower stability of the tetragonal phase in fast-fired industrial coatings when compared with pellet samples is probably related to better homogenization and lower average particle size of the former ones (especially B coatings), and to the promotion of diffusion processes and exposure to kiln atmosphere (in fine layers).

On the other hand, some differences in the reactivity of 3Y–TZP grains towards the glaze were evident as a result of the use of different homogenization procedures (A or B). By comparing Figs. 5a and b, results show that for low Y–TZP contents (typically 10 wt.%) zircon crystallization was kinetically more favorable (more intense zircon XRD peaks) for coatings made with procedure B than for films prepared according to A procedure. Indeed, well-developed zircon crystallization is observed in B2 sample, while A2 sample is highly amorphous. This increasing reactivity observed in B2 sample can be related to the best homogenization conditions and to the particle-size reduction (enhancing the interfacial contact area between the 3Y–TZP grains and the glaze) achieved by the intense milling process carried out before spray-coating operation. However, the effect on t-ZrO_2 stabilization of the distinct homogenization procedure was not so important for higher 3Y–TZP contents ($\geqslant$20 wt.%) and, in both types of samples (A or B), increasing amounts of tetragonal zirconia remained stable in the glaze the higher the 3Y–TZP content. Regarding to monoclinic zirconia, this phase was only present as minor phase in the films. This means that if a relevant martensitic transformation from tetragonal to monoclinic ZrO_2 occurred (induced by yttrium dissolution into the glassy phase and also by the previous grinding process), the solution of the resultant monoclinic phase in the glaze, or its reaction with silica to form zircon are very fast processes.

3.2.2. Microstructural (SEM/EDX) characterization

SEM/EDX analyses of fast-fired industrial coatings are in general accordance with XRD results and give additional valuable information about the dominant processes that govern the development of final ceramic glaze characteristics. SEM micrographs of 3Y–TZP

Table 2
Nomenclature of the samples industrially enameled as film coatings

ZrO_2 phase added to glaze L	Homogenization procedure	Without addition	+10 wt.%	+20 wt.%	+30 wt.%
3Y–TZP	A	A1	A2	A3	A4
	B	B1	B2	B3	B4
ZS-300	A	A1	A5	A6	A7
	B	B1	B5	B6	B7

containing films are shown in Fig. 7a–f. It is easy to confirm the different level of zircon crystallization by comparing micrographs of coatings B2, B3, and B4 with their homologous A2, A3 and A4. Only rare and amorphous ZrO_2 aggregates (as the one shown in Fig. 7a) can be seen by in sample A2, while an important volumetric fraction of elongated prismatic zircon microcrystals (sizes between 1 and 3 μm) may be seen in B2 coating. Also in agreement with XRD results, coarse and more abundant zircon crystals are observed in A3 sample. A detailed view of Fig. 7c shows prismatic zircon crystals (2–3 μm, labeled as A), together with partially solved tetragonal zirconia aggregates (labeled as C) made of sub-micrometric round-shaped grains (around 0.2 μm in size). The volumetric fraction of such aggregates is higher than that of zircon crystals in B3 sample, similarly to what is observed in coatings A4 and B4. In addition, zircon and *t*-ZrO_2 grains may be seen more regularly dispersed or homogenized in B coatings than in A coatings (compare micrographs of Fig. 7e and f), as a result of the intense pre-milling step followed in the former.

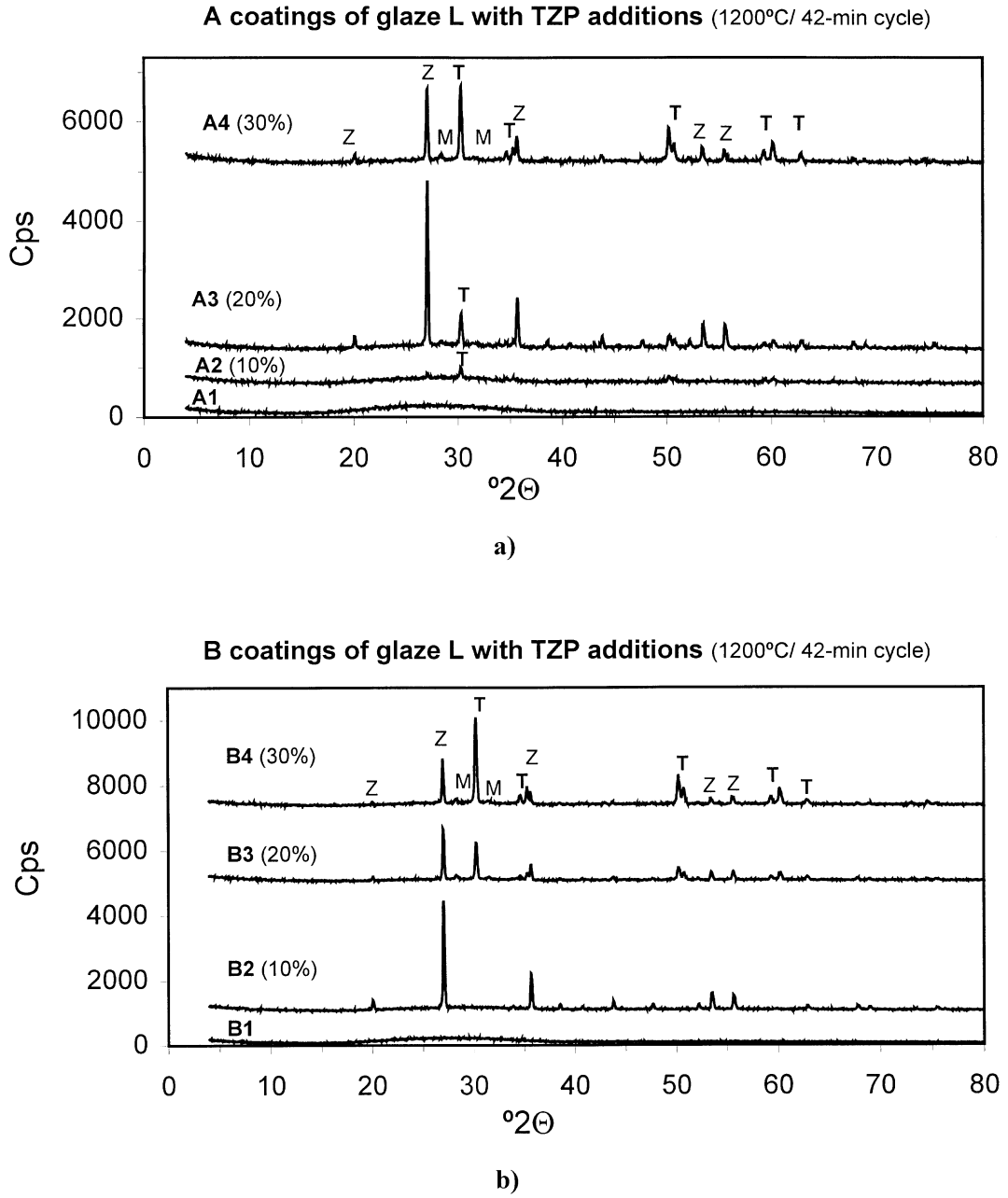

Fig. 5. XRD patterns of coatings of glaze L homogenized with procedure A (a) and B (b) with various additions of 3Y–TZP (10, 20 and 30 wt.%), and fast-fired using a 42-min industrial cycle. Crystalline phases: *T* (tetragonal ZrO_2), *M* (monoclinic ZrO_2), and *Z* ($ZrSiO_4$).

Micrographs of zircon-containing films are shown in Fig. 8a to d. Coarse and heterogeneously shaped zircon particles (from 2–3 to 30 μm) seem to be effectively stable (insoluble) in the glaze. These zircon crystals are also more homogeneously dispersed and present smaller average sizes in B coatings (see Fig. 8e and f): They seem to have a more amorphous character, due to the presence of less sharp edges, and these observations suggest stronger reactivity towards the glaze. The amount and size of stabilized crystals close to the glaze surface, as well as the homogenization level accomplished in the crystal dispersion, are all decisive factors influencing the mechanical and optical properties of the final vitro-crystalline glazes, as shown in the next section.

3.2.3. Mechanical and optical properties

A summary of the measured optical (60°-gloss and whiteness index) and mechanical properties (H_v, K_{IC}, and abrasion resistance) of the industrial coatings is presented in Table 3, together with the dry weight of the glaze layer that was spray-coated on each sample. Standard deviation values on the measured mechanical parameters are included between brackets.

As expected, the addition of 3Y–TZP or zircon crystals increases all the relevant mechanical parameters (H_v

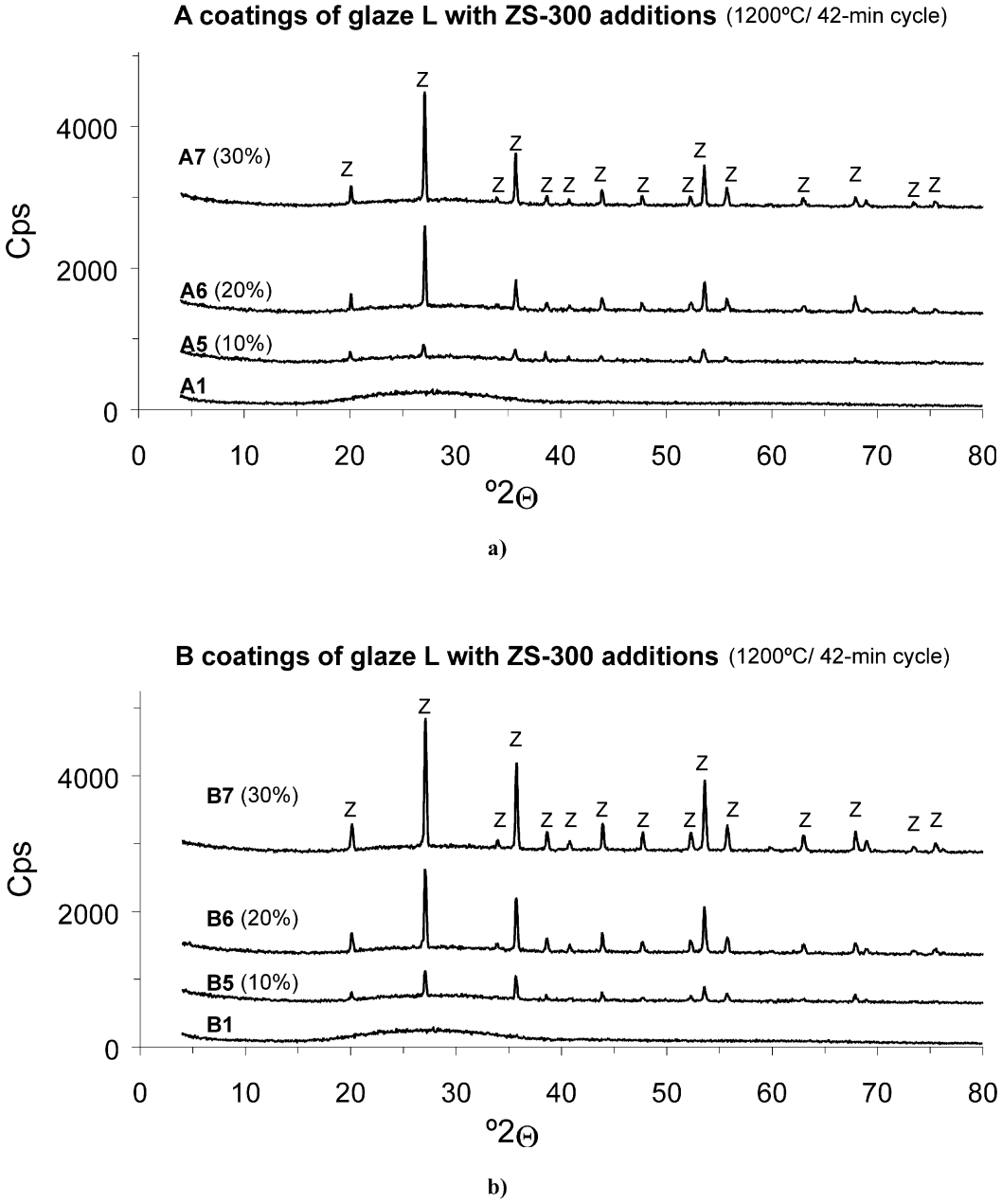

Fig. 6. XRD patterns of coatings of glaze L homogenized with procedure A (a) and B (b) with various additions of ZS-300 (10, 20 and 30 wt.%), and fast-fired using a 42-min industrial cycle. Crystalline phase: *Z* ($ZrSiO_4$).

and K_{IC}), in accordance with increasing formation of reinforcing crystalline phases ($ZrSiO_4$ in samples with zircon addition, and $ZrSiO_4$ plus tetragonal zirconia in samples with 3Y–TZP addition). Moreover, the achieved reinforcement was considerably higher in samples with 3Y–TZP than in samples with zircon addition. On the one hand (see Table 3), H_v values are rather similar, since an equivalent volumetric fraction of reinforcing crystals was obtained in both cases (according to XRD patterns). On the other hand, a substantial increase in fracture toughness is observed in samples with 3Y–TZP (K_{IC} values higher than 2 MPa $m^{1/2}$, except in the A2 sample), since the presence of tetragonal zirconia in these samples allows an additional reinforcement of the ceramic glaze by the transformation-toughening mechanism. The use of different homogenization procedures (A or B) before the spray-coating step did not produce a relevant and clear effect on H_v and K_{IC} values.

Some optical microscope images of Vickers indentations performed on representative samples are shown in Fig. 9. The brittle character of the transparent single firing glaze (L) is denoted in Fig. 9a by the spalling phenomenon caused by an indentation performed with

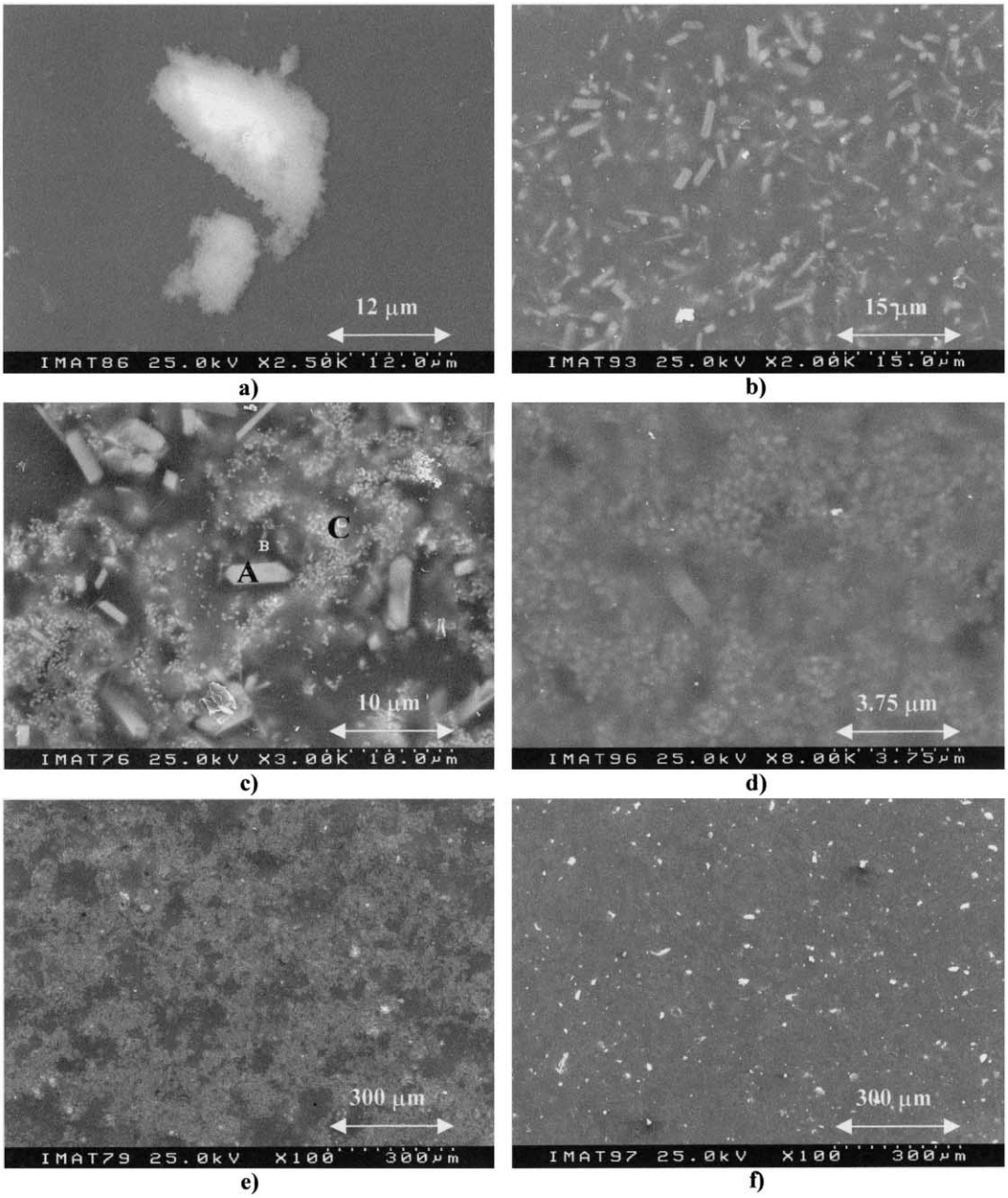

Fig. 7. SEM micrographs (secondary electron detector) of industrial coatings with 3Y–TZP additions: (a) A2 (magnification of 2500), (b) B2 (magnification of 2000), (c) A3 (magnification of 3000), (d) B3 (magnification of 8000), (e) A4 (magnification of 100), and (f) B4 (magnification of 100).

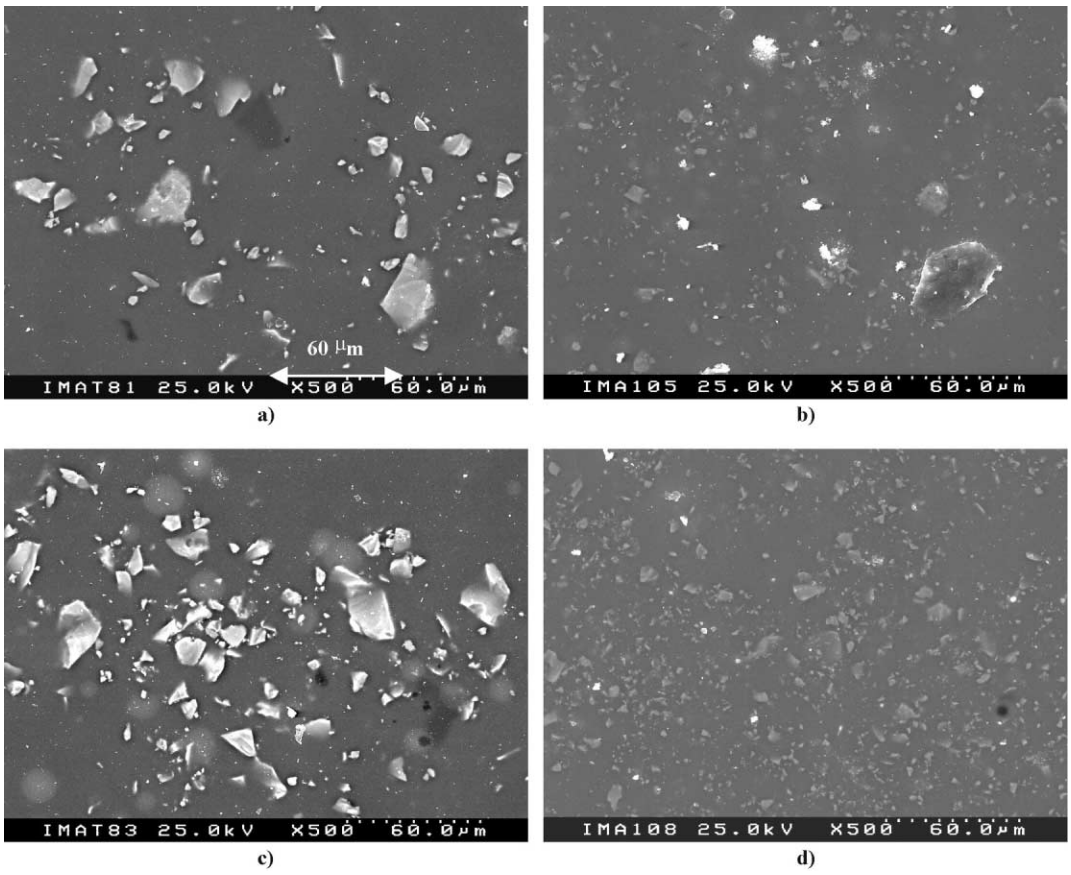

Fig. 8. SEM micrographs (secondary electron detector) of industrial coatings with ZS-300 additions at a magnification of 500: (a) A6, (b) B6, (c) A7, and (d) B7.

Table 3
Weight of glaze layer spray-coated, optical properties (60°-gloss and whiteness index) and values of Vickers microhardness (H_v) fracture toughness (K_{IC}) (standard deviation between parentheses) and PEI abrasion resistance number, corresponding to industrial coatings of glaze L with additions either of 3Y–TZP or of ZS-300 crystals

Enameled sample	Weight of dry glaze spray-coated (g)	Gloss (60°)	Whiteness index[a]	Vickers micro hardness, H_v (GPa)	Toughness, $K_{IC(Niihara)}$ (MPa $m^{1/2}$)	Abrasion resistance (PEI)[b]
Glaze (L)						
A1	56	95	17.8	5.9 (0.4)	1.30 (0.10)	2
B1	52	97	16.4	6.1 (0.5)	1.42 (0.05)	2
L + 3Y–TZP						
A2	54	94	15.3	7.1 (0.5)	1.60 (0.18)	3
B2	60	66	11.0	6.9 (0.4)	2.09 (0.17)	4
A3	55	46	10.3	8.4 (0.5)	2.23 (0.53)	4
B3	52	75	8.6	7.3 (0.2)	2.19 (0.30)	5
A4	66	33	9.7	7.7 (0.8)	2.13 (0.28)	4
B4	52	95	7.9	7.3 (0.4)	2.19 (0.24)	5
L + ZS-300						
A5	59	93	16.1	6.6 (0.4)	1.63 (0.17)	3
B5	82	95	15.1	6.3 (0.2)	1.58 (0.06)	3
A6	61	93	16.2	7.2(0.3)	1.79(0.15)	3
B6	58	96	13.4	7.5 (0.4)	1.88 (0.13)	4
A7	64	92	16.6	7.5(1.2)	1.84 (0.19)	3
B7	61	95	12.8	7.2 (0.3)	1.98 (0.10)	4

[a] Measured according to ASTM 1925 standard.
[b] Measured according to international standard ISO 10545-7.

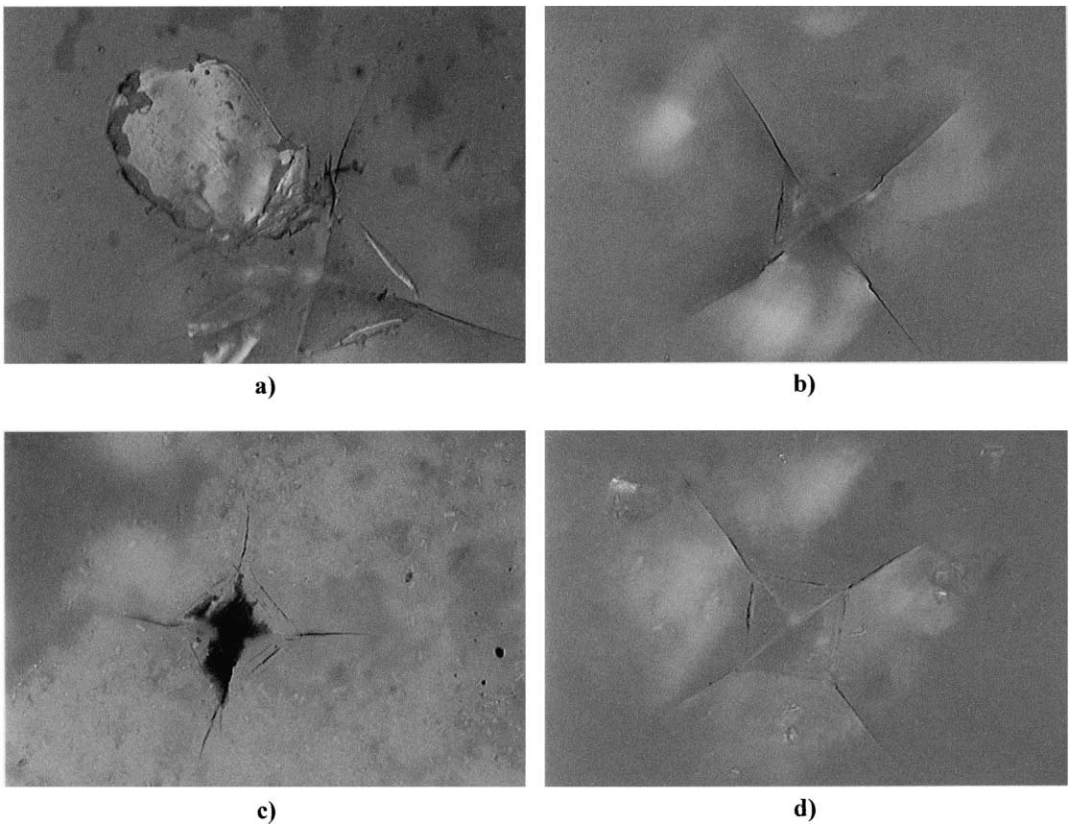

Fig. 9. Optical microscope images of some micro-indentations performed on industrial coatings of glaze L: (a) indentation on sample Al (pure glaze) produced with a load of 4.9 N and observed with lens 5 (0.142 μm pixel), (b) indentation on sample B1 (pure glaze) produced with a load of 9.8 N and observed with lens 4 (0.285 μm/pixel), (c) indentation produced on sample A3 (20% 3Y–TZP) with a load of 9.8 N and observed with lens 4, and (d) indentation on sample A6 (20% ZS-300) produced with a load of 9.8 N and observed with lens 4.

a small load (4.9 N). Fig. 9b corresponds to an indentation on B 1 sample and shows the presence of long cracks that are extended from each apex of the indentation. The improved K_{IC} values of the A3 sample can be explained by the crack-shielding effect caused by the presence of dispersed zircon and/or tetragonal zirconia crystals (see the considerably shorter indentation cracks in Fig. 9c), and also by the possible transformation-toughening mechanism provided by tetragonal zirconia grains. As expected, the mean (average) size of the indentation cracks (1) generated in zircon-containing samples is considerably higher than that observed in samples with equal concentration of 3Y–TZP (see Fig. 9c and d). In fact, the average indentation crack length is 23.2 μm for A3 (20 wt.% 3Y–TZP doped sample), 31.1 μm for A6 (20 wt.% ZS-300 containing sample), and 48.3 μm for Al (pure glaze).

On the other hand, the abrasion resistance of the industrial coatings of glaze L tends to strongly increase by the addition of 3Y–TZP or zircon grains. PEI abrasion number of pure glaze coatings (Al and Bl) is relatively low (PEI = 2), as expected for a transparent, non-crystalline coating, while PEI values of 4 or even of 5 (observed on 3Y–TZP containing samples) are achieved for doped samples. As may be appreciated in Table 3, PET abrasion values of 3Y–TZP containing coatings are always higher than those of homologous ZS-300 doped samples. This result can be attributed to the combined benefic effects of zircon crystallization (as elongated crystals) and of the presence of stabilized tetragonal grains. The wear resistance of ceramic or glass–ceramic materials is governed by fracture and plastic deformation phenomena.[25] According to the literature,[26] martensitic transformation of TZP is mechanically induced while abrading TZP-containing materials. As a result, a compression zone forms in the abraded superficial layer that prevents or makes more difficult the formation and propagation of micro-cracks in the contact surface. Accordingly, martensitic transformation of tetragonal grains can have a positive role on abrasion resistance. B coatings also present higher abrasion resistance values than the homologous A coatings. The improved abrasion resistance of the former must be due to the more homogeneous dispersion of the crystals in these samples. In fact, the volumetric fraction of t-ZrO_2 and/or $ZrSiO_4$ grains in the glaze is rather similar in B and A coatings, according to XRD patterns (except in A2 and B2 samples), and the amount of transformable t-ZrO_2 is not expected to have diminished considerably as a consequence of pre-milling step in B coatings.

Concerning the optical properties (see Table 3), samples become more opaque or whiter (lower whiteness index) with increasing levels of 3Y–TZP or zircon crystals. The opacity of 3Y–TZP containing samples is higher than zircon-doped ones, which can be explained by the higher refraction index of ZrO_2 (2.19–2.20) with respect to that of zircon (1.90–2.05): The corresponding values for common ceramic glaze are about 1.5–1.6. Opacity of B samples is also higher than A. Considering the 60°-gloss measurements, samples with zircon addition exhibited high gloss values (92–96), but similar to those of coatings without crystals addition (95 and 97 for Al and B1 samples, respectively). The gloss of 3Y–TZP doped coatings is strongly affected by the overall amount and relative proportion of zircon and tetragonal zirconia crystalline phases. Sample B4 (30 wt.% 3Y–TZP) shows a very good compromise between highest toughness (2.2 MPa $m^{1/2}$) and abrasion resistance values (PEI 5) and the maintenance of a very high gloss value (95), which suggests the possibility of producing a strong mechanical reinforcement of ceramic glazes by the addition of polycrystalline tetragonal zirconia without compromising the glossy aspect.

4. Conclusions

The insolubility or stability of added tetragonal zirconia in the glaze and/or the occurrence of zircon crystallization was found to be strongly dependent on glaze composition, firing treatment, and on preparation method (uniaxially pressed pellets or film coatings). TZP remains stable in fast-fired pellets, but partial crystallization of prismatic zircon micro-crystals occurred in samples prepared as film coatings, in which diffusion processes are promoted by decreasing the thickness of the glaze and by the exposure to kiln atmosphere. Zircon crystallization in fast-fired glaze coatings is kinetically favored for low 3Y–TZP contents when 3Y–TZP powder is previously ball-milled together with the frit during the homogenization treatment.

Addition of 10–30 wt.% of 3Y–TZP powder to a conventional single-firing glaze, that is industrially enameled (as film coating) onto low-porous floor tiles, produces a significant enhancement of Vickers microhardness (H_v from 6.0 to 8.4 GPa), fracture toughness (K_{IC} from 1.35 to 2.23 MPa $m^{1/2}$), and wear resistance (PEI abrasion number from 2 to 5). This mechanical reinforcement was found to be higher than that due to zircon addition, and must be attributed to the beneficial effect of the stress-induced transformation-toughening mechanism produced by the stabilized tetragonal zirconia.

The opacity of the ceramic glazes increased with the addition of zircon and of 3Y–TZP crystals. Promising results have been obtained for sample B4 (30 wt.% 3Y–TZP), which exhibits the highest toughness (2.2 MPa $m^{1/2}$) and abrasion resistance (PEI 5) values, but still shows a very high gloss value (95). This result corresponds to the achievement of an interesting compromise between mechanical reinforcement of ceramic glazes by inclusion of polycrystalline tetragonal zirconia, and the maintenance of a suitable glossy aspect.

Acknowledgements

M.L. is grateful to the Spanish Direcció General d'Ensenyaments Universitaris i Investigació de la Generalitat Valenciana for the grant concession. G.M. and M.L. acknowledge financial support of CYCYT (MAT98-0392 project). Authors are also grateful to Esmalglass-Portugal S.A. and to Novagres S.A. (Portugal) for their attentive help supplying the materials and industrial equipments in the spray-coating tests, and for the realization of the abrasion resistance measurements.

References

1. Evans, A. G. and Cannon, R. M., Toughening of brittle solids by martensitic transformation. *Acta Metall.,* 1986, **34**(5), 761–800.
2. Tsukuma, K., Kubota, Y. and Tsukidate, T., Thermal and mechanical properties of Y_2O_3-stabilized tetragonal zirconia polycrystals. In *Advances in Ceramics,* Vol. 12*, Science and Technology of Zirconia II*, ed. N. Claussen, M. Rühle and A. Heuer. American Ceramic Society, Columbus, OH, 1984, pp. 382–390.
3. Gupta, T. K., Bechtold, J. H., Kuznicki, R. C., Cadoff, L. H. and Rossing, B. R., Stabilisation of tetragonal phase in polycrystalline zirconia. *J. Mater. Sci.,* 1977, **12**, 2421–2426.
4. Gupta, T. K., Lange, F. F. and Bechtold, J. H., Effect of stress-induced phase transformation on the properties of polycrystalline zirconia containing metastable tetragonal phase. *J. Mater. Sci.,* 1978, **13**, 1464–1470.
5. Garvie, R. C., Hannink, R. H. and Pascoe, R. T., Ceramic steel. *Nature (London),* 1975, **258**, 703–704.
6. Heuer, A. H., Claussen, N., Kriven, M. W. and Rühle, M., Stability of tetragonal ZrO_2 particles in ceramic matrices. *J. Am. Ceram. Soc.,* 1982, **65**(2), 642–650.
7. Nogami, M. and Tomozawa, M., Glass preparation of the ZrO_2 system by the sol-gel process from metal alkoxides. *J. Non-Cryst. Solids,* 1985, **69**, 415–423.
8. Nogami, M. and Tomozawa, M., ZrO_2-transformation-toughened glass-ceramics prepared by the sol-gel process from metal alkoxides. *J. Am. Ceram. Soc.,* 1986, **69**(2), 99–102.
9. Leatherman, L. and Tomozawa, M., Transformation-toughened glass-ceramics. *Am. Ceram. Soc. Bull.,* 1984, **63**(9), 1106.
10. Lima, L., Quinteiro, E. and Ortega, A., Efecto de la presencia de cristales sobre la resistencia al desgaste de vidriados. In *Proceedings of Qualicer'2000, P.GI 17–25*, ed. The Institute of Ceramic Technology (ITC). Cámara Oficial de Comercio, Industria y Navegación, Castellón, Spain, 2000.
11. Descamps, P., Tirlocq, J., Deletter, M. and Cambier, F., El enfoque de composite para el refuerzo de pavimentos cerámicos. In *Acts of Qualicer'2000, P.GI 379–394*, ed. The Institute of Ceramic Technology (ITC). Cámara Oficial de Comercio, Industria y Navegación, Castellón, Spain, 2000.
12. Neilson, G. F., Nucleation and crystallization in ZrO_2-nucleated glass-ceramic systems. In *Advances in Nucleation and Crystal-*

lization in Glasses, ed. L. L. Hench and S. W. Freiman. American Ceramic Society, Columbus, OH, 1971, pp. 73–82.
13. Höche, T., Deckwerth, M. and Rüsselo, C., Partial stabilisation of tetragonal zirconia in oxynitride glass-ceramics. *J. Am. Ceram. Soc.,* 1998, **81**(8), 2029–2036.
14. Generali, E., Baldi, G., Ferrari, A. M., Leonelli, C., Manfredini, T., Siligardi, C. and Pellacani, G. C., Studio di Sistemi Vetroceramici Appartenenti Al Sistema M_2O–CaO–ZrO_2–SiO_2 Come Componenti di smalti per Piastrelle. *Ceramica Informazione,* 1995, **358**, 16–18.
15. Monrós, G., *et al*., Estabilización de circonas para vidriados de pavimento y revestimiento cerámicos de alta K_{IC}. In *Actas de Qualicer' 1998*, ed. The Institute of Ceramic Technology (ITC). Cámara Oficial de Comercio, Industria y Navegación, Castellón, Spain, 1998.
16. Tans, T. and Brungs, M. P., *Phys. Chem. Glasses,* 1980, **21**(4), 133–140.
17. Tans, T. and Brungs, M. P., *Phys. Chem. Glasses,* 1980, **21**(5), 178–183.
18. Zhu, H.-Y., Grinding induced t↔m martensitic transformations and texture in a 12 mol% ceria-doped tetragonal and monoclinic zirconia. *J. Mater. Sci. Lett.,* 1996, **15**, 606–609.
19. Zhu, H.-Y., Correlation between phase transformation and surface texture induced by grinding in tetragonal zirconia polycrystals. *J. Mater. Sci. Lett.,* 1996, **15**, 1126–1128.
20. Virkar, A. V. and Matsumoto, R. L. K., Ferroelastic domain switching as a toughening mechanism in tetragonal zirconia. *J. Am. Ceram. Soc.,* 1986, **69**(10), C-224–C-226.
21. Gross, V. and Swain, M. V., Mechanical properties and microstructure of sintered and hot isostatically pressed yttria partially stabilized zirconia (Y–PSZ). *J. Am. Ceram. Soc.,* 1986, **22**, 1–12.
22. Swain, M. V. and Hannink, R. H. J., Metastability of the martensitic transformation in a 12 mol% ceria-zirconia alloy: II, grinding ztudies. *J. Am. Ceram. Soc.,* 1989, **72**(8), 1358–1364.
23. Bannister, M. J. and Caesar, E. R., *J. Mater. Sci.,* 1988, **23**, 356.
24. Niihara, K., Morena, R. and Hasselman, D. P. H., Evaluation of K_{IC} of brittle solids by the indentation method with low crack-to-indent ratios. *J. Mater. Sci. Lett.,* 1982, **1**, 13–16.
25. Fischer, T. E. and Tomizawa, H., Interaction of microstructure and tribochemistry in the friction and wear of silicon nitride. *Wear,* 1985, **105**(1), 29–45.
26. He, Y., Winnbust, L., Burggraaf, A. J. and Verweij, H., Grain-size dependence of sliding wear in tetragonal zirconia polycrystals. *J. Am. Ceram. Soc.,* 1996, **79**(12), 3090–3096.